Inorg. Chem. **1991**, *30*, 2509–2514

Contribution from the Department of Chemistry and Laboratory for Molecular Structure and Bonding,
Texas A&M University, College Station, Texas 77843, and Department of Chemistry,
University of New Orleans, New Orleans, Louisiana 70148

Oxidative Addition of Halogens to the Quadruple Bond of $Mo_2X_4(dppm)_2$ (X = Cl, I, Br): Synthesis, Structural Characterization, and Magnetic Properties of $Mo_2Cl_4I_2(dppm)_2$, $Mo_2Br_6(dppm)_2$, and $Mo_2I_6(dppm)_2$

F. Albert Cotton,*[,1a] Lee M. Daniels,[1a] Kim R. Dunbar,[1a] Larry R. Falvello,[1a] Charles J. O'Connor,[1b] and Andrew C. Price[1a]

Received November 27, 1990

Oxidative-addition reactions of Y_2 (Y = Cl, Br, I) to the quadruply bonded complexes $Mo_2X_4(dppm)_2$ (X = Cl, Br, I) produce the corresponding edge-sharing bioctahedral molecules $Mo_2X_4Y_2(dppm)_2$ in high yield. All nine of these compounds are now available and have been investigated by infrared and UV-visible spectroscopy as well as by electrochemical methods. Structural determinations of three of them, $Mo_2Cl_4I_2(dppm)_2$ (**2**), $Mo_2Br_6(dppm)_2$ (**4**), and $Mo_2I_6(dppm)_2$ (**8**), have been carried out, although in the case of **4** refinement is incomplete. Pertinent crystal data are as follows: for **2**, $P\bar{1}$, $a = 9.922$ (3) Å, $b = 13.013$ (5) Å, $c = 12.152$ (5) Å, $\alpha = 93.31$ (3)°, $\beta = 107.06$ (2)°, $\gamma = 108.63$ (2)°, $V = 1402$ (1) Å^3, $Z = 1$; for **4**, $P\bar{1}$, $a = 16.069$ (6) Å, $b = 20.994$ (6) Å, $c = 10.756$ (6) Å, $\alpha = 102.43$ (3)°, $\beta = 106.99$ (4)°, $\gamma = 77.52$ (3)°, $V = 3343$ (3) Å^3, $Z = 2$; for **8**, $P2_1/n$, $a = 16.194$ (8) Å, $b = 11.090$ (2) Å, $c = 20.574$ (7) Å, $\beta = 108.72$ (4) °, $V = 3499$ (6) Å^3, $Z = 2$. Compound **2** has bridging Cl atoms, and each terminal position is occupied by a 1:1 mixture of Cl and I. The Mo–Mo distances in **2**, **4**, **8**, and $Mo_2Cl_6(dppm)_2$ are respectively 2.827 (1), 2.879 (2), 3.061 (1), and 2.789 (1) Å. Magnetic susceptibility data over a temperature range 5–300 K have been fitted to an expression that allows evaluation of the gap between a ground singlet state and a low triplet state. For **2** the gap is >1750 cm^{-1}, while for the other three compounds whose structures are known, $Mo_2X_6(dppm)_2$, X = Cl, Br, and I, the S–T gap is 1100–1400 cm^{-1}, indicating that both direct M–M coupling and indirect coupling across the μ-X atoms play a part.

Introduction

For several years we have been investigating the oxidative-addition chemistry of metal–metal multiple bonds as they occur in various M_2L_8 complexes. For example, coordinatively unsaturated molecules of the type $M_2Cl_4(L\text{-}L)_2$ (M = Mo, W; L-L = dppm, dppe) react with oxidizing reagents such as halogens,[2] disulfides,[3] and diselenides[2c,4] to form edge-sharing bioctahedral complexes. One of the goals in this work is the designed synthesis of target molecules with specific ligand sets. We reasoned that if the incoming substrate, Y_2, oxidatively adds across the metal–metal bond, we would have a method of selectively introducing specific entities into the bridging positions. The structural and magnetic properties of a series of related complexes synthesized in this manner would then allow further insight into the importance of size and identity of bridging groups in determining the extent of M–M interaction.

We now report several new halogen-containing edge-sharing bioctahedral dimolybdenum(III) compounds prepared by the oxidative-addition route. The X-ray structure and variable-temperature magnetic susceptibility data for three of the compounds, viz., $Mo_2Cl_4I_2(dppm)_2$, $Mo_2Br_6(dppm)_2$, and $Mo_2I_6(dppm)_2$, will also be presented and discussed.

Experimental Section

Starting Materials. $Mo_2I_4(dppm)_2$ was prepared by a procedure involving the reaction between $Mo_2(O_2CCH_3)_4$ and dppm in the presence of trimethylsilyl iodide.[5] $Mo_2Cl_4(dppm)_2$[6] and $Mo_2Br_4(dppm)_2$[7] were prepared according to literature methods. Bis(diphenylphosphino)methane (dppm) was purchased from Strem Chemicals and used without further purification. Iodine and bromine were obtained from Aldrich; the iodine was purified by sublimation and the bromine was used as received. Toluene was freshly distilled from sodium/potassium benzophenone ketyl, and dichloromethane was distilled from P_4O_{10}.

Reaction Procedures. All operations were carried out under an atmosphere of dry argon by using standard Schlenk-line techniques.

Synthesis of $Mo_2X_6(dppm)_2$ Complexes by Oxidative-Addition Reactions. A. $Mo_2Cl_4X_2(dppm)_2$ Compounds (X = Cl, Br, I). (i) $Mo_2Cl_6(dppm)_2$. The preparation of this compound was previously reported by the oxidative-addition method.[2c]

(ii) $Mo_2Cl_4Br_2(dppm)_2$ (1). A solution of 0.20 g (0.181 mmol) of $Mo_2Cl_4(dppm)_2$ in 30 mL of CH_2Cl_2 was treated with 1.8 mL of a freshly prepared stock solution of $Br_2(l)$ in CH_2Cl_2 (0.1 M). Upon addition of the Br_2, the green solution turned red. The reaction was stirred at room temperature for an additional 5 min, upon which time 20 mL of diethyl ether was added to induce crystallization. A red microcrystalline product was collected by suction filtration in air, washed with diethyl ether, and dried. Yield: 0.21 g (92%). Anal. Calcd for $Br_2C_{50}H_{44}Cl_4P_4Mo_2$: C, 47.57; H, 3.51; Br, 12.66. Found: C, 47.20; H, 3.72; Br, 12.04. IR spectrum, CsI plates (Nujol mull), cm^{-1}; 1580 w, 1565 w, 1480 s, 1430 vs, 1325 w, 1305 w, 1185 w, 1155 w, 1090 s, 1025 w, 995 w, 775 s, 735 vs, 720 m, 690 vs, 520 s, 510 m, 480 m, 360 m, 320 w.

(iii) $Mo_2Cl_4I_2(dppm)_2$ (2). In a typical reaction, 0.092 g (0.36 mmol) of I_2 was added to a 0.40-g (0.363-mmol) sample of $Mo_2Cl_4(dppm)_2$ dissolved in 30 mL of CH_2Cl_2. An immediate color change from green to red-purple occurred with no further change after stirring for 5 h at room temperature. Benzene (20 mL) was added to the reaction solution, and the mixture was refrigerated at 0 °C for 2 days. A crop of dark purple crystals was filtered off, washed with diethyl ether, and dried in vacuo. The filtrate was treated with additional benzene to give more product. Combined yield: 0.45 g (91%). Anal. Calcd for $C_{50}H_{44}I_2Cl_4P_4Mo_2$: C, 44.28; H, 3.27. Found: C, 44.63; H, 3.58. IR spectrum, CsI plates (Nujol mull), cm^{-1}: 1585 w, 1570 w, 1485 m, 1435 s, 1190 w, 1160 w, 995 s, 1030 w, 1000 w, 780 m, 740 vs, 720 m, 690 s, 525 m, 510 w, 485 m, 365 m, 330 m.

B. $Mo_2Br_4X_2(dppm)_2$ Compounds (X = Cl, Br, I). (i) $Mo_2Br_4Cl_2(dppm)_2$ (3). A small quantity of $Cl_2(g)$ was bubbled into a chloroform suspension of $Mo_2Br_4(dppm)_2$ (0.110 g, 0.086 mmol). A reaction immediately ensued, resulting in a color change from green to red-purple. The solution was filtered through Celite into a Schlenk tube and layered with diethyl ether. A crop of dark red crystals was obtained after 1 day at room temperature. Yield: 0.10 g (86%). Anal. Calcd for $Br_4C_{50}H_{44}Cl_2P_4Mo_2$: C, 44.44, H, 3.28; Cl, 5.25. Found: C, 44.68; H, 3.49; Cl, 5.16. IR spectrum, CsI plates (Nujol mull), cm^{-1}: 1580 w, 1565 w, 1480 m, 1430 s, 1300 w, 1180 w, 1155 w, 1125 w, 1090 s, 1025 w, 995 w, 770 s, 740 m, 730 vs, 712 m, 685 s, 520 m, 505 w, 475 m, 450 w, 420 w, 350 w, 315 s.

(ii) $Mo_2Br_6(dppm)_2$ (4). A sample of $Mo_2Br_4(dppm)_2$ (0.400 g, 0.312 mmol) was dissolved in CH_2Cl_2 (30 mL) and treated with liquid Br_2 (1 equiv, 17 μL). The solution was stirred at room temperature for 12 h and filtered to yield a bright green solid (0.310 g) and a red-green dichroic filtrate. Addition of diethyl ether to the filtrate produced 0.10 g of additional solid. The combined solids were dried in vacuo. Yield: 0.41 g (91%). Anal. Calcd for $Br_6C_{50}H_{44}P_4Mo_2$: C, 41.70; H, 3.08; Br,

---

(1) (a) Texas A&M University. (b) University of New Orleans.

(2) (a) Agaskar, P. A.; Cotton, F. A.; Dunbar, K. R.; Falvello, L. R.; O'Connor, C. J. *Inorg. Chem.* **1987**, *26*, 1305. (b) Canich, J. A. M.; Cotton, F. A.; Daniels, L. M.; Lewis, D. B. *Inorg. Chem.* **1987**, *26*, 4046. (c) Canich, J. A. M.; Cotton, F. A.; Dunbar, K. R.; Falvello, L. R. *Inorg. Chem.* **1988**, *27*, 804.

(3) (a) Cotton, F. A.; Powell, G. L. *J. Am. Chem. Soc.* **1984**, *106*, 3372. (b) Cotton, F. A.; Diebold, M. P.; O'Connor, C. J.; Powell, G. L. *J. Am. Chem. Soc.* **1985**, *107*, 7438.

(4) Cotton, F. A.; Dunbar, K. R. *Inorg. Chem.* **1987**, *26*, 1305.

(5) Cotton, F. A.; Dunbar, K. R.; Poli, R. *Inorg. Chem.* **1986**, *25*, 3700.

(6) Best, S. A.; Smith, T. J. Walton, R. A. *Inorg. Chem.* **1978**, *17*, 99.

(7) Campbell, F. L.; Cotton, F. A.; Powell, G. L. *Inorg. Chem.* **1984**, *23*, 4222.

0020-1669/91/1330-2509$02.50/0

33.29. Found: C, 41.35; H, 3.63; Br, 32.85. IR spectrum, KBr plates (Nujol mull), cm^{-1}: 1570 w, 1185 w, 1120 w, 1095 m, 775 m, 735 s, 715 w, 690 m, 520 w, 505 w, 478 w, 450 w, 420 w.

(iii) $Mo_2Br_4I_2(dppm)_2$ (5). A 0.22-g quantity of $Mo_2Br_4(dppm)_2$ (0.172 mmol) was dissolved in CH_2Cl_2 (30 mL), and I_2(s) (0.044 g, 0.17 mmol) was added to the solution at room temperature. After being stirred for 1 h, the bright green solution was filtered under nitrogen, reduced in volume to ~10 mL, and chilled to −10 °C for 12 h. A green microcrystalline product was collected, washed with diethyl ether, and dried. Yield: 0.25 g (91%). Anal. Calcd for $Br_4C_{50}H_{44}I_2P_4Mo_2$: C, 39.15; H, 2.89. Found: C, 39.32; H, 2.32. IR spectrum, KBr plates (Nujol mull), cm^{-1}: 1575 w, 1565 w, 1480 m, 1425 s, 1300 w, 1185 w, 1155 w, 1090 s, 1025 w, 995 w, 770 m, 730 vs, 710 m, 685 s, 520 m, 505 w, 480 m.

C. $Mo_2I_4X_2(dppm)_2$ Compounds (X = Cl, Br, I). (i) $Mo_2I_4Cl_2(dppm)_2$ (6). A 0.20-g quantity of $Mo_2I_4(dppm)_2$ (0.136 mmol) was dissolved in a mixture of 15 mL of CH_2Cl_2 and 5 mL of toluene to which was added 3.5 mL of Cl_2(g) via a syringe. The color of the solution changed from green to red and finally to red-brown within 0.5 h at room temperature. A red crystalline product was obtained by chilling the flask to −10 °C for 24 h. Yield: 0.19 g (90%). Anal. Calcd for $C_{50}H_{44}Cl_2I_4P_4Mo_2$: C, 39.02; H, 2.88. Found: C, 38.79; H, 2.64. IR spectrum, KBr plates (Nujol mull), cm^{-1}: 1570 w, 1190 w, 1155 w, 1093 m, 1030 w, 1000 w, 768 m, 738 s, 688 m, 525 w, 507 w, 483 w, 450 w, 420 w.

(ii) $Mo_2I_4Br_2(dppm)_2$ (7). To a dichloromethane solution (30 mL) of $Mo_2I_4(dppm)_2$ (0.25 g, 0.170 mmol) was added 1 equiv of Br_2(l) in CH_2Cl_2 (1.45 mL of a 0.095 M solution). A color change from green-brown to dark olive green occurred within 5 min. The reaction was stirred at room temperature for 1 h, reduced in volume to 10 mL, and chilled to −10 °C for 8 h. An olive green precipitate was collected by filtration in air. Additional product was obtained by addition of diethyl ether to the filtrate. The combined solids were washed with diethyl ether and dried. Yield: 0.24 g (87%). Anal. Calcd for $Br_2C_{50}H_{44}I_4P_4Mo_2$: C, 36.89; H, 2.72. Found: C, 36.69; H, 2.71. IR spectrum, CsI plates (Nujol mull), cm^{-1}: 1580 w, 1565 w, 1475 m, 1425 s, 1345 w, 1325 w, 1300 w, 1185 w, 1153 w, 1130 w, 987 s, 1025 w, 995 w, 770 s, 730 vs, 710 m, 682 s, 520 s, 505 w, 475 m, 445 w, 420 w, 350 w.

(iii) $Mo_2I_6(dppm)_2$ (8). A dichloromethane solution (10 mL) of $Mo_2I_4(dppm)_2$ (0.20 g, 0.136 mmol) was treated with 1 equiv (0.035 g) of elemental iodine. The green solution immediately turned orange-brown with no further change of color after stirring at room temperature for 3 h. The reaction solution was filtered through Celite, treated with 15 mL of toluene, and refrigerated at −10 °C for 3 days. A crop of dark brown crystals was filtered off, washed with cold toluene, and dried under reduced pressure. Yield: 0.19 g (83%). Anal. Calcd for $C_{50}H_{44}I_6P_4Mo_2$: C, 34.87; H, 2.57. Found: C, 34.39; H, 2.52. IR spectrum, CsI plates (Nujol mull), cm^{-1}: 1575 w, 1674 w, 1475 m, 1422 m, 1220 w, 1150 w, 1090 m, 1020 w, 995 m, 763 m, 730 s, 705 m, 685 s, 520 m, 505 w, 475 m.

Preparation of Single Crystals. Suitable crystals of $Mo_2I_6(dppm)_2 \cdot CH_2Cl_2 \cdot C_7H_8$ and $Mo_2Cl_4I_2(dppm)_2 \cdot C_6H_6$ were obtained by slow diffusion of toluene into dichloromethane solutions of the compounds at −10 °C. Small dark red-green dichroic crystals of $Mo_2Br_6(dppm)_2 \cdot 4CHCl_3$ were obtained by slow evaporation of a chloroform solution of the compound. The crystals were found to lose interstitial solvent rapidly.

Physical Measurements. Infrared spectra were recorded on a Perkin-Elmer 783 spectrophotometer by using Nujol mulls between CsI or KBr plates, while visible spectra were recorded as CH_2Cl_2 solutions in quartz cells on a Cary 17 UV-vis spectrophotometer. Electrochemical measurements were carried out on dichloromethane solutions that contained 0.1 M tetra-*n*-butylammonium hexafluorophosphate (n-Bu_4NPF_6 or TBAH) as supporting electrolyte. $E_{1/2}$ values, determined as $(E_{p,a} + E_{p,c})/2$, were referenced to the silver/silver chloride (Ag/AgCl) electrode at room temperature. Under our experimental conditions, $E_{1/2} = +0.47$ V vs Ag/AgCl for the ferrocenium/ferrocene couple. Voltammetric experiments were performed on a Bioanalytical Systems Inc. Model 100 electrochemical analyzer. Polycrystalline samples of the complexes were measured with a Model 905 superconducting SQUID susceptometer from SHE Corp. operating at a measuring field of 5.00 kOe. Microanalyses were performed by Galbraith Laboratories, Inc., Knoxville, TN.

X-ray Structure Analysis. Data Collection and Reduction. Block-shaped crystals of $Mo_2Br_6(dppm)_2$ and $Mo_2I_6(dppm)_2$ were mounted at the ends of glass fibers and placed in a cold stream of N_2 at −60 °C (4) and −106 °C (8) on the goniometer of an Enraf-Nonius CAD-4 diffractometer. Data collection for $Mo_2Cl_4I_2(dppm)_2$ was carried out at room temperature on a Syntex $P\bar{1}$ diffractometer. The procedures employed for data collection have been described previously.[8] The unit cell parameters and orientation matrix were refined by a least-squares fit to the positions of 25 reflections.

Table I. Crystallographic Data for Compounds **2**, **4**, and **8**

formula	$Mo_2Cl_4I_2P_4$-$C_{56}H_{50}$	$Mo_2Cl_{12}Br_6P_4$-$C_{54}H_{48}$	$Mo_2Cl_2I_6P_4$-$C_{58}H_{54}$
fw	1434.41	1917.64	1899.18
space group	$P\bar{1}$ (No. 2)	$P\bar{1}$ (No. 2)	$P2_1/n$ (No. 14)
a, Å	9.922 (3)	16.069 (6)	16.194 (8)
b, Å	13.013 (5)	20.994 (6)	11.090 (2)
c, Å	12.152 (5)	10.756 (6)	20.574 (7)
α, deg	93.31 (3)	102.43 (3)	90.000
β, deg	107.06 (2)	106.99 (4)	108.72 (4)
γ, deg	108.63 (2)	77.52 (3)	90.000
V, Å^3	1402 (1)	3343 (3)	3499 (6)
Z	1	2	2
D_{calc}, g/cm^3	1.700	1.905	1.802
μ(Mo Kα), cm^{-1}	18.67	47.7	63.37
radiation (λ_α, Å)		Mo Kα (0.71073)	
temp, °C	20 ± 1	−60 ± 1	−106 ± 1
transm factor	0.998, 0.724	0.999, 0.629	0.998, 0.615
$R(F_o)$	0.0734	0.0760	0.042
$R_w(F_o)$	0.0880	0.0999	0.059

The ω–2θ scan technique was used to gather data points in the range $4 \le 2\theta \le 45°$ (50° in the case of **4**). Three check reflections monitored throughout data collection displayed no significant gain or loss in intensity. Data reduction was carried out by using well-established computational procedures.[9] The data were corrected for Lorentz and polarization effects, and azimuthal scans (ψ scans) of reflections having an Eulerian angle χ near 90° were used as the basis for an empirical absorption correction.[10]

Structure Solution and Refinement. $Mo_2Cl_4I_2(dppm)_2 \cdot C_6H_6$. The position of the Mo atom was determined from the Patterson map. Following least-squares refinement of the metal atom parameters, a difference Fourier map revealed the atoms of the coordination sphere. A Cl atom refined well in the position bridging the two metal atoms, but the atoms trans to the bridging Cl atoms would refine as neither Cl nor I alone. Atoms modeled as half-Cl and half-I refined well in these positions, although the Mo–X (X = Cl, I) distances are not expected to be equivalent. A model was therefore defined in which half-occupancy atoms of I and Cl were placed at reasonable distances from the Mo atom. The occupancy ratio Cl:I at each disordered coordination site was allowed to vary in subsequent least-squares cycles. In order to maintain meaningful Mo–I and Mo–Cl bond distances, typical values for Mo–I and Mo–Cl were added as *observations* in the refinement calculations. Subsequent difference Fourier maps revealed the remainder of the carbon atoms, including an ill-defined benzene molecule about an inversion center. Final least-squares refinement gave discrepancy indices of $R = 0.0743$ and $R_w = 0.0880$. Table I lists other data pertaining to structure refinement. Table II lists the atomic coordinates.

$Mo_2Br_6(dppm)_2 \cdot 4CHCl_3$ (4). The structure was solved by the direct-methods algorithm in SHELXS-86,[11] which gave the positions of the two independent molybdenum atoms and the phosphorus and the bromine atoms. The unit cell was found to consist of two independent $Mo_2Br_6(dppm)_2$ molecules, each residing on an inversion center. All carbon atoms were located by an alternating series of difference Fourier maps and least-squares refinement cycles. The asymmetric unit was also found to contain several molecules of solvent, but because of a combination, presumably, of both disorder and partial occupancy, we found it impossible to model this part of the structure satisfactorily. This, in turn, led to such high figures of merit [$R = 0.0760$; $R_w = 0.0999$; quality-of-fit = 2.932] that we do not consider it worthwhile to report this structure in as much detail as those of **2** and **8**. However, the principal dimensions, e.g., the Mo–Mo distance, that are of importance here are doubtless reliable, albeit with somewhat higher uncertainties than may be inferred from the esd's given. The positional parameters, a drawing of the molecule, and a complete list of bond angles and distances are available in the supplementary material.

$Mo_2I_6(dppm)_2 \cdot CH_2Cl_2 \cdot C_7H_8$ (8). The monoclinic symmetry was confirmed by axial photography, and the space group was determined to be

---

(8) Cotton, F. A.; Frenz, B. A.; Deganello, G.; Shaver, A. *J. Organomet. Chem.* **1973**, *50*, 227.

(9) Data processing and refinement was done on a VAX-11/780 computer with programs from the package VAXSDP.

(10) North, A. C. T.; Phillips, D. C.; Mathews, F. S. *Acta Crystallogr., Sect. A: Cryst. Phys., Diffr., Theor. Gen. Crystallogr.* **1968**, *A24*, 351.

(11) Sheldrick, G. M. SHELXS-86. Insitute für Anorganische Chemie der Universität, Göttingen, FRG, 1986.

(12) Walker, N.; Stuart, D. *Acta Crystallogr., Sect. A: Found. Crystallogr.* **1983**, *39*, 158.

Table II. Positional and Equivalent Isotropic Thermal Parameters and Their Estimated Standard Deviations for $Mo_2Cl_4I_2(dppm)_2$ (**2**)

atom	*x*	*y*	*z*	*B*,[a] Å^2
Mo	0.0603 (1)	−0.02764 (9)	0.11001 (8)	2.42 (3)
I(1)	0.2163 (4)	−0.1623 (4)	0.1912 (3)	3.64 (9)
I(2)	0.0728 (5)	0.0211 (5)	0.3356 (5)	3.3 (1)
Cl(1)	0.213 (2)	−0.137 (2)	0.197 (2)	4.6 (6)*
Cl(2)	0.081 (2)	0.015 (1)	0.313 (1)	4.0 (4)*
Cl(3)	0.0982 (3)	−0.0813 (3)	−0.0680 (3)	3.05 (9)
P(1)	0.3071 (3)	0.1424 (3)	0.1632 (3)	2.72 (9)
P(2)	−0.1846 (3)	−0.1954 (3)	0.0810 (3)	2.80 (9)
C(1)	0.345 (1)	0.174 (1)	0.028 (1)	3.1 (4)
C(2)	0.329 (1)	0.275 (1)	0.241 (1)	3.2 (4)
C(3)	0.217 (2)	0.286 (1)	0.285 (1)	3.6 (4)
C(4)	0.243 (2)	0.389 (1)	0.344 (1)	4.8 (5)
C(5)	0.375 (2)	0.481 (1)	0.358 (1)	5.4 (6)
C(6)	0.481 (2)	0.466 (1)	0.314 (1)	5.2 (5)
C(7)	0.459 (1)	0.363 (1)	0.258 (1)	4.4 (5)
C(8)	0.478 (1)	0.121 (1)	0.252 (1)	3.3 (4)
C(9)	0.499 (1)	0.118 (1)	0.368 (1)	3.9 (4)
C(10)	0.626 (2)	0.102 (1)	0.443 (1)	4.4 (5)
C(11)	0.733 (2)	0.095 (1)	0.400 (1)	4.4 (5)
C(12)	0.718 (2)	0.100 (2)	0.285 (1)	5.5 (6)
C(13)	0.589 (1)	0.116 (1)	0.208 (1)	4.3 (5)
C(14)	−0.198 (1)	−0.336 (1)	0.035 (1)	3.1 (4)
C(15)	−0.114 (1)	−0.355 (1)	−0.032 (1)	3.5 (4)
C(16)	−0.132 (2)	−0.461 (1)	−0.075 (1)	4.4 (5)
C(17)	−0.238 (2)	−0.553 (2)	−0.051 (2)	6.2 (6)
C(18)	−0.320 (2)	−0.534 (2)	0.021 (2)	6.1 (6)
C(19)	−0.300 (2)	−0.424 (1)	0.063 (1)	4.9 (5)
C(20)	−0.243 (1)	−0.208 (1)	0.209 (1)	3.1 (4)
C(21)	−0.370 (2)	−0.193 (1)	0.218 (1)	3.9 (4)
C(22)	−0.410 (2)	−0.207 (1)	0.319 (1)	5.0 (6)
C(23)	−0.316 (2)	−0.233 (1)	0.414 (1)	4.8 (5)
C(24)	−0.186 (2)	−0.248 (1)	0.405 (1)	4.7 (5)
C(25)	−0.151 (2)	−0.237 (1)	0.305 (1)	4.1 (5)
C(26)	0.073 (5)	0.592 (4)	0.443 (6)	16 (2)
C(27)	0.133 (6)	0.595 (4)	0.556 (6)	15 (3)
C(28)	0.088 (6)	0.522 (6)	0.617 (5)	18 (2)

[a] *B* values for anisotropically refined atoms are given in the form of the isotropic equivalent displacement parameter defined as $(4/3)[a^2\beta_{11} + b^2\beta_{22} + c^2\beta_{33} + ab(\cos\gamma)\beta_{12} + ac(\cos\beta)\beta_{13} + bc(\cos\alpha)\beta_{23}]$. Asterisks indicate *B* values of atoms refined isotropically.

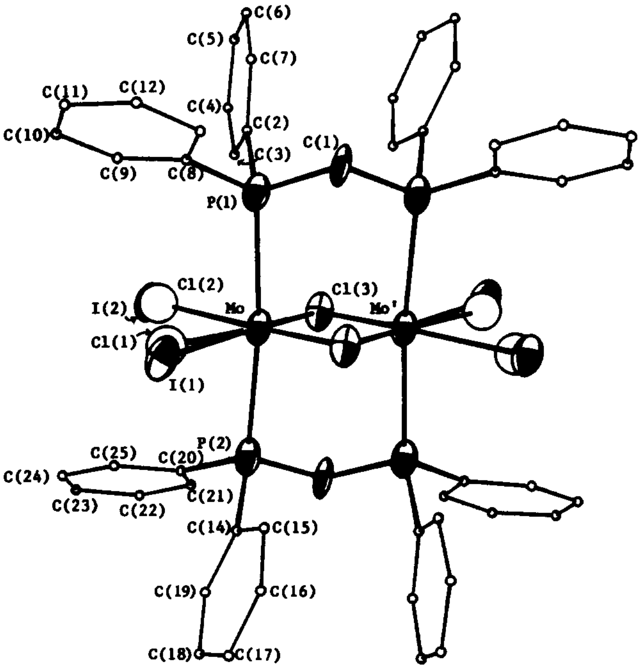

Figure 1. ORTEP diagram of $Mo_2Cl_4I_2(dppm)_2$ (**2**), showing atoms as 50% probability ellipsoids. Carbon atoms of the phenyl groups are shown as spheres of arbitrary radii.

Table III. Positional and Equivalent Isotropic Thermal Parameters and Their Estimated Standard Deviations for $Mo_2I_6(dppm)_2$ (**8**)

atom	*x*	*y*	*z*	*B*,[a] Å^2
Mo(1)	1.00903 (4)	0.04749 (7)	0.57181 (3)	1.27 (1)
I(1)	0.92234 (3)	0.16145 (5)	0.45333 (3)	1.47 (1)
I(2)	1.06669 (4)	−0.02361 (5)	0.70908 (3)	1.91 (1)
I(3)	0.97214 (4)	0.26074 (5)	0.62928 (3)	2.02 (1)
P(1)	1.1353 (1)	0.0604 (2)	0.4323 (1)	2.14 (5)
P(2)	1.1609 (1)	0.1394 (2)	0.5813 (1)	2.00 (5)
C(1)	1.2115 (6)	0.0705 (8)	0.5216 (4)	1.9 (2)
C(2)	1.1423 (5)	0.2158 (8)	0.4003 (4)	1.8 (2)
C(3)	1.2265 (6)	0.2629 (9)	0.4154 (5)	2.7 (2)
C(4)	1.2377 (7)	0.379 (1)	0.3914 (5)	3.1 (2)
C(5)	1.1635 (6)	0.4472 (9)	0.3543 (5)	2.7 (2)
C(6)	1.0813 (7)	0.3978 (9)	0.3415 (5)	2.8 (2)
C(7)	1.0707 (6)	0.2812 (8)	0.3642 (4)	2.1 (2)
C(8)	1.1979 (6)	−0.0248 (9)	0.3884 (5)	2.5 (2)
C(9)	1.1856 (7)	0.006 (1)	0.3188 (5)	3.7 (3)
C(10)	1.2301 (8)	−0.068 (1)	0.2844 (5)	4.9 (3)
C(11)	1.2813 (8)	−0.162 (1)	0.3160 (7)	6.2 (4)
C(12)	1.2910 (8)	−0.193 (1)	0.3839 (7)	5.8 (3)
C(13)	1.2500 (7)	−0.125 (1)	0.4207 (5)	3.6 (3)
C(14)	1.2415 (5)	0.1034 (8)	0.6656 (4)	1.8 (2)
C(15)	1.2455 (7)	0.1806 (9)	0.7194 (5)	2.8 (2)
C(16)	1.2993 (7)	0.153 (1)	0.7855 (5)	3.7 (3)
C(17)	1.3469 (7)	0.046 (1)	0.7972 (5)	3.3 (2)
C(18)	1.3426 (7)	−0.029 (1)	0.7427 (5)	3.4 (2)
C(19)	1.2887 (6)	−0.0011 (9)	0.6767 (5)	2.3 (2)
C(20)	1.1806 (6)	0.2979 (8)	0.5701 (4)	1.7 (2)
C(21)	1.2650 (6)	0.3446 (8)	0.5961 (5)	2.4 (2)
C(22)	1.2820 (7)	0.465 (1)	0.5836 (6)	3.5 (3)
C(23)	1.2155 (7)	0.5377 (9)	0.5445 (5)	3.0 (2)
C(24)	1.1297 (6)	0.4920 (8)	0.5180 (5)	2.2 (2)
C(25)	1.1120 (6)	0.3727 (8)	0.5297 (4)	2.0 (2)
Cl(1)	0.9147 (3)	0.7494 (4)	0.1149 (3)	8.2 (1)
Cl(2)	1.5961 (4)	−0.1812 (7)	0.6752 (3)	12.7 (2)
C(26)	1.513 (1)	−0.260 (2)	0.6842 (8)	10.2 (6)
C(27)	0.472 (1)	0.560 (2)	0.387 (2)	15.6 (9)
C(28)	1.4991 (9)	−0.325 (2)	0.399 (1)	11.6 (6)
C(29)	1.5247 (9)	−0.270 (2)	0.4679 (8)	7.1 (4)
C(30)	1.547 (1)	−0.155 (2)	0.473 (1)	10.3 (6)
C(31)	1.548 (1)	−0.081 (2)	0.425 (1)	13.2 (7)
C(32)	1.5281 (9)	−0.126 (2)	0.3648 (8)	8.3 (5)
C(33)	1.5047 (8)	−0.251 (1)	0.3436 (8)	6.2 (4)

[a] *B* values for anisotropically refined atoms are given in the form of the equivalent isotropic displacement parameter defined as $(4/3)[a^2\beta_{11} + b^2\beta_{22} + c^2\beta_{33} + ab(\cos\gamma)\beta_{12} + ac(\cos\beta)\beta_{13} + bc(\cos\alpha)\beta_{23}]$.

$P2_1/n$ on the basis of systematic absences. The structure was solved by using the direct-methods program MULTAN,[13] which gave the position of the unique molybdenum atom. The remaining non-hydrogen atoms were located by using an alternating series of difference Fourier maps and least-squares refinement cycles. In addition to the molecule of chemical interest, the asymmetric unit contains one CH_2Cl_2 and one C_7H_8 interstitial solvent molecule. In the end, 370 parameters were fitted to 4185 observations. The refinement finished with satisfactory figures of merit as listed in Table I. Table III lists atomic coordinates and equivalent isotropic thermal parameters, while selected bond distances and angles may be found in Table IV.

Discussion

Structures. The structural results for compounds **2** and **8** are given in detail in Table IV and Figures 1 and 2. Corresponding results for **4** are available as supplementary material. Table V gives a few main results for **4**. Compounds **4** and **8** complete the series of homohalogeno molecules, $Mo_2X_6(dppm)_2$. In fact, this set of three compounds is the first such complete structurally characterized triad of edge-sharing bioctahedral compounds.[14] The three structures, for X = Cl, Br, and I, show a steady increase in the Mo–Mo distance, viz., 2.789 (1),[15] 2.879 (2), and 3.061 (1) Å. It seems reasonable to attribute this increase primarily to the increasing size of the bridging atoms, but it must be noted

---

(13) As implemented in the commercial package SDP/V.

(14) Cotton, F. A. *Polyhedron* **1987**, *6*, 667.

(15) Chakravarty, A. R.; Cotton, F. A.; Diebold, M. P.; Lewis, D. B.; Roth, W. J. *J. Am. Chem. Soc.* **1986**, *108*, 971.

Table IV. Selected Bond Distances and Angles and their Estimated Standard Deviations for Compounds **2** and **8**

Bond Distances (Å)			
$Mo_2Cl_4I_2(dppm)_2$ (**2**)			
Mo–Mo′	2.827 (1)	Mo–Cl(3)	2.404 (4)
Mo–I(1)	2.734 (6)	Mo–Cl(3)′	2.404 (4)
Mo–I(2)	2.736 (6)	Mo–P(1)	2.599 (3)
Mo–Cl(1)	2.46 (3)	Mo–P(2)	2.611 (3)
Mo–Cl(2)	2.44 (1)		
$Mo_2I_6(dppm)_2$ (**8**)			
Mo(1)–Mo(1)′	3.061 (1)	Mo(1)–I(3)	2.793 (1)
Mo(1)–I(1)	2.704 (1)	Mo(1)–P(1)	2.603 (2)
Mo(1)–I(1)′	2.691 (1)	Mo(1)–P(2)	2.611 (2)
Mo(1)–I(2)	2.789 (1)		
Bond Angles (deg)			
$Mo_2Cl_4I_2(dppm)_2$ (**2**)			
Mo′–Mo–I(1)	135.6 (1)	I(1)–Mo–Cl(3)′	81.9 (1)
Mo′–Mo–I(2)	138.2 (1)	I(1)–Mo–Cl(3)	168.8 (1)
Mo′–Mo–Cl(1)	139.0 (6)	I(1)–Mo–P(1)	91.9 (1)
Mo′–Mo–Cl(2)	140.1 (5)	I(1)–Mo–P(2)	86.9 (1)
Mo′–Mo–Cl(3)	53.00 (9)	I(2)–Mo–Cl(1)	82.8 (6)
Mo′–Mo–Cl(3)′	53.97 (8)	I(2)–Mo–Cl(2)	2.2 (5)
Mo′–Mo–P(1)	92.51 (8)	I(2)–Mo–Cl(3)′	167.1 (2)
Mo′–Mo–P(2)	92.70 (8)	I(2)–Mo–Cl(3)	84.4 (2)
I(1)–Mo–I(2)	86.1 (2)	I(2)–Mo–P(1)	85.7 (1)
I(1)–Mo–Cl(1)	4.6 (5)	I(2)–Mo–P(2)	88.0 (1)
I(1)–Mo–Cl(2)	84.3 (5)	Mo–Cl(3)–Mo′	72.0 (1)
$Mo_2I_6(dppm)_2$ (**8**)			
Mo(1)′–Mo(1)–I(1)	55.23 (2)	I(1)–Mo(1)–P(1)	89.13 (5)
Mo(1)′–Mo(1)–I(1)′	55.64 (2)	I(1)–Mo(1)–P(2)	95.12 (5)
Mo(1)′–Mo(1)–I(2)	141.03 (3)	I(2)–Mo(1)–I(3)	81.85 (3)
Mo(1)′–Mo(1)–I(3)	137.12 (3)	I(2)–Mo(1)–P(1)	84.72 (5)
Mo(1)′–Mo(1)–P(1)	90.24 (6)	I(2)–Mo(1)–P(2)	91.90 (5)
Mo(1)′–Mo(1)–P(2)	90.16 (6)	I(3)–Mo(1)–P(1)	95.22 (6)
I(1)–Mo(1)–I(1)′	110.86 (3)	I(3)–Mo(1)–P(2)	87.83 (6)
I(1)–Mo(1)–I(2)	162.40 (4)	Mo(1)–I(1)–Mo(1)′	69.12 (2)
I(1)–Mo(1)–I(3)	82.31 (3)		

Table V. Selected Bond Distances and Angles and Their Estimated Standard Deviations for $Mo_2Br_6(dppm)_2$ (**4**)

Distances (Å)			
Mo(1)–Mo(1)′	2.879 (2)	Mo(2)–Mo(2)′	2.854 (1)
Mo(1)–Br(1)	2.520 (1)	Mo(2)–Br(4)	2.509 (1)
Mo(1)–Br(1)′	2.512 (2)	Mo(2)–Br(4)′	2.524 (1)
Mo(1)–Br(2)	2.546 (2)	Mo(2)–Br(5)	2.554 (1)
Mo(1)–Br(3)	2.572 (1)	Mo(2)–Br(6)	2.542 (1)
Mo(1)–P(1)	2.580 (3)	Mo(2)–P(3)	2.581 (3)
Mo(1)–P(2)	2.583 (3)	Mo(2)–P(4)	2.590 (3)
Angles (deg)			
Mo(1)′–Mo(1)–Br(1)	54.97 (4)	Mo(2)′–Mo(2)–Br(4)′	55.19 (3)
Mo(1)′–Mo(1)–Br(1)′	55.22 (4)	Mo(2)′–Mo(2)–Br(5)	140.23 (4)
Mo(1)′–Mo(1)–Br(2)	138.58 (4)	Mo(2)′–Mo(2)–Br(6)	136.89 (4)
Mo(1)′–Mo(1)–Br(3)	138.64 (5)	Mo(2)′–Mo(2)–P(3)	90.86 (7)
Mo(1)′–Mo(1)–P(1)	91.25 (9)	Mo(2)′–Mo(2)–P(4)	92.61 (7)
Mo(1)′–Mo(1)–P(2)	92.36 (8)	Br(4)–Mo(2)–Br(4)′	110.89 (4)
Br(1)–Mo(1)–Br(1)′	110.20 (6)	Br(4)–Mo(2)–Br(5)	85.07 (4)
Br(1)–Mo(1)–Br(2)	83.87 (5)	Br(4)–Mo(2)–Br(6)	165.44 (6)
Br(1)–Mo(1)–Br(3)	165.05 (6)	Br(4)–Mo(2)–P(3)	91.58 (7)
Br(1)–Mo(1)–P(1)	86.81 (7)	Br(4)–Mo(2)–P(4)	85.04 (7)
Br(1)–Mo(1)–P(2)	95.06 (7)	Br(4)′–Mo(2)–Br(5)	162.69 (4)
Br(1)′–Mo(1)–Br(2)	165.11 (5)	Br(4)′–Mo(2)–Br(6)	82.17 (4)
Br(1)′–Mo(1)–Br(3)	83.75 (5)	Br(4)′–Mo(2)–P(3)	89.40 (7)
Br(1)′–Mo(1)–P(1)	94.63 (8)	Br(4)′–Mo(2)–P(4)	97.90 (7)
Br(1)′–Mo(1)–P(2)	87.64 (8)	Br(5)–Mo(2)–Br(6)	82.87 (4)
Br(2)–Mo(1)–Br(3)	82.78 (5)	Br(5)–Mo(2)–P(3)	83.30 (7)
Br(2)–Mo(1)–P(1)	90.90 (9)	Br(5)–Mo(2)–P(4)	89.90 (7)
Br(2)–Mo(1)–P(2)	86.23 (9)	Br(6)–Mo(2)–P(3)	95.09 (7)
Br(3)–Mo(1)–P(1)	86.69 (7)	Br(6)–Mo(2)–P(4)	86.80 (7)
Br(3)–Mo(1)–P(2)	90.77 (7)	P(3)–Mo(2)–P(4)	172.65 (9)
P(1)–Mo(1)–P(2)	176.4 (1)	Mo(1)–Br(1)–Mo(1)′	69.80 (4)
Mo(2)′–Mo(2)–Br(4)	55.70 (3)	Mo(2)–Br(4)–Mo(2)′	69.11 (4)

that the nature of the terminal atoms is not entirely irrelevant, as shown by the comparison of $Mo_2(\mu\text{-}Cl)_2Cl_4(dppm)_2$ with $Mo_2(\mu\text{-}Cl)_2Cl_2I_2(dppm)_2$, where the replacement of two terminal Cl atoms by I atoms is accompanied by an increase of 0.038 (2) Å in the Mo–Mo distance.

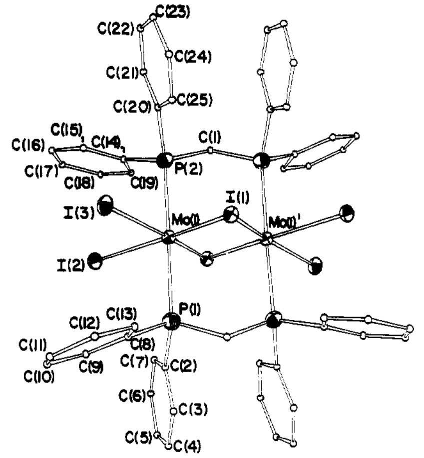

Figure 2. ORTEP diagram of $Mo_2I_6(dppm)_2$ (**8**), showing atoms as 50% probability ellipsoids. Carbon atoms of the phenyl groups are shown as spheres of arbitrary radii.

Scheme I. $Mo_2X_4(dppm)_2$ Reactions

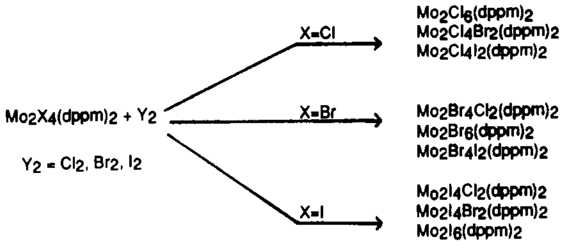

The structure of $Mo_2(\mu\text{-}Cl)_2Cl_2I_2(dppm)_2$ (**2**) requires some comment. The best model we could find for refining the crystal structure was one in which each of the two crystallographically independent terminal halogen positions is occupied by a 1:1 mixture of Cl and I. What does this imply about the structure of an individual molecule? Only that one of three structures (or indeed two of them or all three of them) is randomly disordered on the crystallographic site of $\bar{1}$ symmetry. The three structures in question (showing only the central $Mo_2Cl_4I_2$ plane) are A, B, and C. While "chemical intuition" may tend to discount one or another altogether and perhaps favor another, the structural results in themselves do not distinguish among them; there is no other experimental evidence yet available to do so.

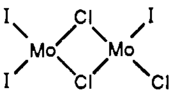

A

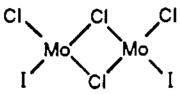

B

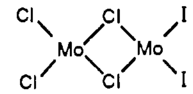

C

Syntheses. With the synthetic results reported here, we now have efficient synthetic access to all nine of the $Mo_2X_4Y_2(dppm)_2$ molecules with X and Y each independently being Cl, Br, or I (see Scheme I). However, for the six mixed species there is a question of isomers. Even if we assume that the two bridging atoms are of the same type (which need not be so, but probably is) and we also neglect the possibility of geometric isomers of the sort just discussed for **2**, we still have in the remaining cases an important question: Which halogen occupies the bridging position and why? It *may* be that regardless of the mechanism by which the addition of Y_2 to $Mo_2X_4(dppm)_2$ occurs, there will be subsequent processes of halogen scrambling that allow a thermodynamically preferred arrangement to be reached. On the other hand, the product may be determined by the mechanism of the addition process. All of these interrelated questions of structure, mechanism, and thermodynamic stability are the subject of continuing work.

Magnetic Properties. The magnetic properties of the three new compounds as well as those of $Mo_2Cl_6(dppm)_2$ have been determined and are presented in Table VI. Results from previous

Table VI. Parameters from the Best Fit of Eq 1 to the Magnetic Data for $Mo_2X_6(L\text{-}L)_2$ Compounds[a]

complex	g	$E(^3B_{1u})$, cm^{-1}	$E(^1B_{1u})$, cm^{-1}	TIP, emu/mol	% impurity
$Mo_2Cl_6(dppm)_2$	2.00	1200	4000	0.000 31	0.83
$Mo_2Cl_4I_2(dppm)_2$		>1750			
$Mo_2Br_6(dppm)_2$	1.99	1408	3000	0.013 7	0.010
$Mo_2I_6(dppm)_2$	1.99	1128	2100	0.000 80	0.005
$Mo_2Cl_6(dppe)_2$[16]	1.99	941	1600	0.000 24	0.017
$Mo_2Cl_4(\mu\text{-}SEt)_2(dto)_2$[17]	2.0	680	965	0.000 226	0.18

[a] Equation 1 is as follows: $\chi = (Ng^2\mu_B{}^2/kT)[2e^{-x_1}/(1 + 3e^{-x_1} + e^{-x_2} + e^{-x_3})]$.

Table VII. Summary of Electrochemical and Electronic Spectral Data for the $Mo_2X_6(dppm)_2$ Compounds

	$E_{1/2}$, V vs Ag/AgCl[a]				
complex	oxidn(2)	oxidn(1)	redn(1)	redn(2)	λ_{max}, nm[b]
$Mo_2Cl_6(dppm)_2$			-0.50^c		290, 325 (sh), 395, 530, 752
$Mo_2Cl_4Br_2(dppm)_2$			-0.63		400 (sh), 540, 690, 765
$Mo_2Cl_4I_2(dppm)_2$	$+1.40^d$	$+1.23^d$	-0.55		460 (sh), 580, 715
$Mo_2Br_4Cl_2(dppm)_2$		$+1.31^d$	-0.50	-0.93^c	360, 410 (sh), 565, 770
$Mo_2Br_6(dppm)_2$			-0.55	-1.25^c	310, 362, 425, 590
$Mo_2Br_4I_2(dppm)_2$			-0.70^c		280, 360, 625, 750
$Mo_2I_4Cl_2(dppm)_2$		$+0.64^d$	-0.58^c		310 (sh), 407, 455 (sh), 520 (sh), 700
$Mo_2I_4Br_2(dppm)_2$	$+1.28^d$	$+1.10^d$	-0.50^c	-1.15^c	320 (sh), 400 (sh), 460 (sh), 625, 680
$Mo_2I_6(dppm)_2$	$+0.70^e$	$+0.38^e$	-0.47^c	-0.95^c	350, 420, 460, 525, 550 (sh), 710

[a] Measured in 0.1 M TBAH/CH_2Cl_2 with a scan rate (v) of 200 mV s^{-1} at a Pt-disk electrode. [b] Samples were run as dichloromethane solutions in quartz cells; molar absorptivity values were not obtained. [c] $E_{p,c}$ (irreversible reduction). [d] $E_{p,a}$ (irreversible oxidation). [e] Chemical product waves.

studies of two related compounds are also given for comparison. The treatment of the data and the meaning of the terms in the equation for χ as a function of temperature are explained in earlier papers.[16,17] As discussed previously,[2] in these molecules we expect the orbitals pertaining to Mo–Mo bonding to increase in energy in the order σ, π, δ^*, δ, π^*, σ^*, with the first three being each doubly occupied. However, the HOMO–LUMO gap, the energy difference between δ^* and δ, is not expected to be large and indeed in the two previous cases included in Table VI the magnetic behavior showed that from the $\sigma^2\pi^2\delta^{*2}$ ground state a triplet state based on the $\sigma^2\pi^2\delta^*\delta$ configuration was thermally accessible enough to influence the magnetic susceptibility measurably.

In the present compounds the singlet–triplet (S–T) separations are all larger. For $Mo_2Cl_4I_2(dppm)_2$ only a lower limit can be set, since no deviation from simple diamagnetic behavior was observed. In the other three cases the S–T separations are in the range of 1100–1400 cm^{-1}, without any significant correlation with the Mo–Mo distances. The value of ca. 1200 cm^{-1} for $Mo_2Cl_6(dppm)_2$ is probably subject to an uncertainty of at least 200 cm^{-1} owing to the relatively large percentage of paramagnetic impurity, while for the other two $Mo_2X_6(dppm)_2$ compounds an uncertainty of perhaps 100 cm^{-1} seems realistic. Thus, despite the rapidly increasing Mo–Mo distance as we move through the series with X = Cl, Br, and I, the S–T separation remains roughly constant.

We believe that these results can best be understood by attributing the S–T separations to the operation of two effects: (1) direct Mo–Mo bonding, which will lead to a rapid reduction in the S–T gap as Mo–Mo distances increase in the series Cl, Br, and I, and (2) superexchange coupling across the halogen atom bridges, which would tend to increase in the series Cl, Br, and I. The net result of (2) increasing the gap while (1) decreases it could account for the fact that the observed result is a substantially invariant gap.

Other Properties. Electrochemical and visible spectral results for all nine compounds are presented in Table VII. All of the compounds show one or more oxidation and/or reduction processes, but the majority are irreversible, presumably because they lead to qualitative changes in structure. The only reversible redox processes are one-electron reductions in four cases. It is not surprising that addition of one electron to an essentially nonbonding δ orbital is reversible, but it is a little surprising that it is not reversible in all cases. The general irreversibility of oxidation may be due mainly to the increased charge on the metal atoms, which would weaken the σ and π bonding. It is not to be expected that loss of a δ^* electron would, in itself, seriously destablize the structure.

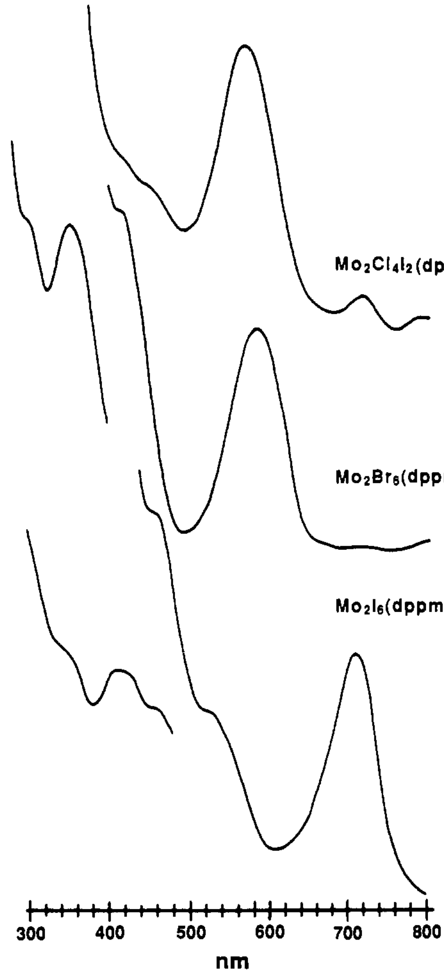

Figure 3. UV-visible spectra for compounds 2, 4, and 8.

The visible spectra (several of which are shown in Figure 3)

---

(16) Agaskar, P. A.; Cotton, F. A.; Dunbar, K. R.; Falvello, L. R.; O'Connor, C. J. *Inorg. Chem.* **1987**, *26*, 4051.

(17) Cotton, F. A.; Diebold, M. P.; O'Connor, C. J.; Powell, G. L. *J. Am. Chem. Soc.* **1985**, *107*, 7438.

are complicated and will be the subject of a future report.

Acknowledgment. We thank the National Science Foundation for financial support.

Supplementary Material Available: Full tables of crystal parameters and results of data collection and refinement, bond distances, bond angles, and anisotropic displacement parameters for **2**, **4**, and **8** and a table of positional and thermal parameters and ORTEP drawings for **4** (35 pages); tables of observed and calculated structure factors (77 pages). Ordering information is given on any current masthead page.

Contribution from the School of Chemical Sciences
and Materials Research Laboratory, University of Illinois, Urbana, Illinois 61801

Synthesis and Structure of [M(*N*-methylimidazole)$_6$]S$_8$ (M = Mn, Fe, Ni, Mg). Polysulfide Salts Prepared by the Reaction *N*-Methylimidazole + Metal Powder + Sulfur

Somanath Dev, Emannuel Ramli, Thomas B. Rauchfuss,* and Scott R. Wilson

Received November 20, 1990

Powdered magnesium, manganese, iron, and nickel were found to dissolve in *N*-methylimidazole (*N*-MeIm) solutions of elemental sulfur to give red-colored salts [M(*N*-MeIm)$_6$]S$_8$. The structure of the nickel complex was determined by single-crystal X-ray diffraction. The compound crystallizes in the triclinic space group $P\bar{1}$ with a = 8.027 (5) Å, b = 10.785 (2) Å, c = 11.531 (2) Å, α = 112.79 (2)°, β = 92.35 (3)°, γ = 96.11 (3)°, Z = 1. The structure analysis revealed a centrosymmetric cation that is analogous to other hexakis(imidazole) complexes. The compounds [M(*N*-MeIm)$_6$]S$_8$ are rare examples of polysulfide salts of transition-metal complexes. The IR spectra of the new compounds were analyzed by comparison with samples of [M(*N*-MeIm)$_6$]I$_2$ that were prepared by the reaction of the metal powders with iodine in *N*-MeIm solution.

Introduction

We have recently shown that donor solvents such as pyridine and *N*-alkylimidazoles promote the reaction of metal powders with elemental sulfur.[1] These reactions can be described using the notation L–M–X, where L is the donor ligand, M is a metal powder, and X is the oxidant. The L–M–X process can be viewed as a chemically well-behaved and synthetically useful form of oxidative corrosion.

Previous examples of L–M–X reactions are the syntheses of divalent acetonitrile complexes of the type [M(MeCN)$_6$](BF$_4$)$_2$ by the reaction of acetonitrile suspensions of metal powders with nitrosonium salts.[2-5] It has also been reported that several first-row transition metals dissolve in dimethyl sulfoxide (DMSO) solutions of sulfur dioxide to give salts of the type [M(DMSO)$_6$]X where X = SO_4^{2-} and $S_2O_7^{2-}$.[6] Manganese powder has long been known to react with an ether solution of iodine giving MnI$_2$.[7] Pohl and co-workers have synthesized salts of the anionic clusters $Fe_6S_6I_6^{2-}$ and $Fe_8S_6I_8^{2-}$ by the reaction I$^-$/Fe/S$_8$ + I$_2$, in weakly coordinating solvents.[8] The Lewis base in these processes is the iodide anion, and both sulfur and iodine serve as oxidants.

The reaction L/Cu/S$_8$ affords clusters of the type Cu$_4$(S$_5$)$_2$L$_4$ (L = *N*-MeIm and substituted pyridines) which, aside from their interesting structure, are noteworthy as intermediates in the conversion of copper metal to CuS. The L/Cu/S$_8$ reaction works for both pyridines and especially for *N*-alkylimidazoles, whereas the dissolution of zinc could only be effected in hot *N*-MeIm. The *N*-MeIm/Zn/S$_8$ and *N*-MeIm/Zn/Se$_n$ reactions afford tetrahedral coordination complexes of the type ZnS$_6$(*N*-MeIm)$_2$ and ZnSe$_4$(*N*-MeIm)$_2$.[9]

In this paper, we describe the products of the *N*-MeIm/M/S$_8$ reaction for M = Mn, Fe, Ni, and Mg. This investigation has resulted in the preparation of a series of polysulfide salts of metal complexes.

Results

Synthesis of [M(*N*-MeIm)$_6$]S$_8$. Suspensions of magnesium, manganese, iron, and nickel powders dissolve over a period of several days in a solution of elemental sulfur in *N*-MeIm. After a typical reaction period, the reaction mixtures consisted of a red precipitate and a red solution. The red precipitate proved to have the formula [M(*N*-MeIm)$_6$]S$_8$, and the red solution yielded the same product after layering with diethyl ether. For M = Mg, Mn, and Fe these reactions proceeded quantitatively at 80 °C in 1 h (eq 1). Nickel powder dissolves more slowly in the *N*-

$$\mathrm{M} + \mathrm{S_8} + 6N\text{-MeIm} \rightarrow [\mathrm{M}(N\text{-MeIm})_6]\mathrm{S_8} \qquad (1)$$

$$\mathrm{M} = \mathrm{Mg, Mn, Fe, Ni}$$

MeIm/S$_8$ solution, but the resulting red solution yielded [Ni(*N*-MeIm)$_6$]S$_8$ in 35% yield. The yield and rate of the nickel reaction can be increased by conducting the reaction at 50 °C, but the yields are not quantitative. Cobalt, chromium, vanadium, and titanium do not dissolve in *N*-MeIm/S$_8$ at room temperature even after several days. Cobalt metal reacts with *N*-MeIm solutions of elemental sulfur to give an insoluble solid that was not characterized. It was found that a suspension of sulfur in 33% aqueous ammonia was unreactive toward nickel powder. Solutions of sulfur in pyridine, acetonitrile, 3-methylpyrazole, *N*-methylmorpholine, ethylenediamine, and 2,2′-bipyridine/DMF were also found to be uneffective in this dissolving metal reaction. Moreover, small amounts of iodine did not accelerate the reactions nor did iodine induce the activation of chromium or cobalt.

The new compounds give highly conductive solutions in *N*-MeIm and the conductivities are comparable. They are soluble in DMF, but preliminary studies show that dissolution is accompanied by displacement of some of the *N*-MeIm ligands. For example, the manganese compound gives a turbid solution in

---

(1) Ramli, E.; Rauchfuss, T. B.; Stern, C. L. *J. Am. Chem. Soc.* **1990**, *112*, 4043.

(2) Mn, Fe, Co, Cu, and Zn + NOBF$_4$: Hathaway, B. J.; Holah, D. G.; Underhill, A. E. *J. Chem. Soc.* **1962**, 2444.

(3) Pd + NOBF$_4$: Schramm, R. F.; Wayland, B. B. *J. Chem. Soc., Chem. Commun.* **1968**, 898.

(4) Mn, Co, and Ni + halogens in MeCN: Hathaway, B. J.; Holah, D. G. *J. Chem. Soc.* **1964**, 2400.

(5) Cu +NOClO$_4$: Hathaway, B. J.; Underhill, A. E. *J. Chem. Soc.* **1960**, 3705.

(6) Harrison, W. D.; Gill, J. B.; Goodall, D. C. *J. Chem. Soc., Dalton Trans.* **1978**, 1431. Harrison, W. D.; Gill, J. B.; Goodall, D. C. *J. Chem. Soc., Dalton Trans.* **1979**, 847. Gill, J. B.; Goodall, D. C.; Jefferys, B. *J. Chem. Soc., Dalton Trans.* **1986**, 2603. Graham, N. K.; Gill, J. B.; Goodall, D. C. *J. Chem. Soc., Dalton Trans.* **1978**, 1363.

(7) Mn + X$_2$: Ducelliez, F. *Bull. Soc. Chim. Fr.* **1913**, *13*, 815. Ducelliez, F.; Raynaud, A. *Bull. Soc. Chim. Fr.* **1914**, *15*, 273. Related syntheses from metal powders and hydrogen halides, CrX$_2$(THF)$_2$ (X = Cl, Br) and MnBr$_2$: Larkworthy, L. F.; Richardson, M. H. O. *Chem. Ind.* **1974**, 164. Winter, G. *Aust. J. Chem.* **1968**, *21*, 2864.

(8) (NR$_4$)$_3$Fe$_8$S$_6$I$_8$: Pohl, S.; Saak, W. *Angew. Chem., Int. Ed. Engl.* **1984**, *23*, 907. *Angew. Chem.* **1984**, *96*, 886. (NR$_4$)$_2$Fe$_6$S$_6$I$_6$: Saak, W.; Henkel, G.; Pohl, S. *Angew. Chem., Int. Ed. Engl.* **1984**, *23*, 150. *Angew. Chem.* **1984**, *96*, 153. (NR$_4$)$_2$Fe$_4$S$_4$I$_4$ and (NR$_4$)$_2$Fe$_2$S$_2$I$_4$: Saak, W.; Pohl, S. *Z. Naturforsch.* **1985**, *40B*, 1105.

(9) Dev, S.; Ramli, E.; Rauchfuss, T. B.; Wilson, S. R. *J. Am. Chem. Soc.* **1990**, *112*, 6385.

0020-1669/91/1330-2514$02.50/0 © 1991 American Chemical Society